Supercell calculations for transition metal impurities in palladium

1993 J. Phys.: Condens. Matter 5 5099

(http://iopscience.iop.org/0953-8984/5/29/007)

J. Phys.: Condens. Matter 5 (1993) 5099–5112. Printed in the UK

Supercell calculations for transition metal impurities in palladium

P Mohn and K Schwarz

Technical University of Vienna, A-1060 Getreidemarkt 9/158, Vienna, Austria

Received 5 January 1993, in final form 5 April 1993

Abstract. The electronic and magnetic behaviour of transition metal impurities is simulated by performing *ab initio* band structure calculations assuming ordered supercells with the composition $Pd_{31}TM$ (TM = Cr, Mn, Fe, Co, Ni). The results show the formation of narrow spin-split impurity bands originating from the TM with magnetic moments M_{TM} deviating from the Slater–Pauling curve. Due to the high susceptibility of the Pd host the TM atom polarizes the surrounding Pd atoms (with M_{Pd}) causing the 'giant moments' when all the magnetic moment is attributed to the TM impurity. This polarization is described by a covalent polarization (CP) model, which we use for explaining both the change in sign of the Pd polarization in the TM series between Cr and Mn, and the linear dependence of the ratio M_{Pd}/M_{TM} on the number of valence electrons of the TM. In addition, we estimate the Curie temperature by treating the localized TM moments in terms of a Weiss mean-field model and the itinerant electrons of the Pd host having spin fluctuations.

1. *Introduction*

There has been a long lasting interest in the magnetic and electronic properties of transition metal (TM) impurities in palladium. Early investigations (Bozorth *et al* 1961) led to magnetic moments up to 11 μ_B per Co atom, when Co is substituted in a Pd host, a phenomenon for which the term 'giant moment' was introduced. This behaviour was explained by assuming that the Co magnetic moment remains at about 1.7 μ_B as in pure Co and the 12 next nearest Pd neighbours each carry about 0.6 μ_B (corresponding to a complete polarization of the 0.6 holes in the 4d band) and thus provide the required polarization, while more distant Pd atoms remain almost unpolarized. Neutron scattering experiments on Fe and Co impurities (Low and Holden 1966) confirmed the large values of the total moment per impurity atom, but found larger moments of 3.5 μ_B and 2.1 μ_B at the Fe and Co impurities, respectively. In addition, the neutron data revealed a polarization around each impurity extending up to 200 rather than 12 Pd atoms. The experimental situation has been reviewed by Nieuwenhuys (1975), but contradicting results, concerning the size of the polarization cloud around the impurity, still appear in the literature (Ododo 1985).

The rapid growth of supercomputer power and the development of efficient methods made it possible to start theoretical investigations of the band structure and the magnetic properties of such systems. Delley *et al* (1982) reported on results they obtained from their molecular cluster approach using up to 55 atoms investigating Fe impurities in Ag or Pd hosts, denoted as Fe**Ag** and Fe**Pd**. These results are in good agreement with LMTO supercell calculations (Delley *et al* 1983) with up to 27 atoms per unit cell, for which different atomic arrangements were assumed. Both investigations find that the magnetic

0953-8984/93/295099+14$07.50

moment of the impurity is independent of the cluster (cell) size and is in agreement with the neutron diffraction data obtained by Cable *et al* (1965).

Oswald *et al* (1986) reported self-consistent calculations for the same 3d impurities as in the present paper, employing the Korringa–Kohn–Rostoker Green-function method for the infinite crystal. In their calculation, perturbations of the first three neighbouring Pd shells were taken into account and their results will be compared in detail to the supercell results presented here.

2. The electronic structure of the Pd host

The electronic structure and the resulting magnetic properties of Pd are unique among the transition metals. The Fermi energy E_F lies at the top of the 4d bands (figure 1) and falls in a region of very high density of states (DOS). This gives rise to an enhancement of the susceptibility by a factor 7–8 (Jarlborg and Freeman 1981). The temperature dependence of the susceptibility shows a maximum, which led Wohlfarth and Rhodes (1962) to argue that Pd could be a possible candidate for a metamagnetic system. However, recent band structure calculations by the present authors (1992) find no metamagnetic transition, but a strong deviation from the usual paramagnetic behaviour, which has been explained by means of spin fluctuations yielding the experimentally observed maximum (at $T_m = 90$ K) in the susceptibility. This model (Wagner 1989, Mohn *et al* 1989, 1991, Mohn and Schwarz 1992) associates this maximum with the extremely large susceptibility and the small number of holes (unoccupied states) in the 4d bands combined with the presence of spin fluctuations which can be treated within a Ginzburg–Landau approach. Recently an analogous calculation was reported by Kirchner *et al* (1992). Some of the concepts used in these papers are needed for the present work and thus are briefly summarized below.

We have calculated the electronic structure of the FCC Pd host using the fixed spin moment (FSM) method (Williams *et al* 1984, Schwarz and Mohn 1984). From these total energy results (for constant volume) we derive the Landau coefficients A, B, and C of the free energy:

$$F = (A/2)M^2 + (B/4)M^4 + (C/6)M^6. \tag{2.1}$$

At the equilibrium volume the respective values of these Landau coefficients are $A = 0.0136$, $B = -0.0825$, $C = 0.727$, where the units are such that on entering the magnetic moment in Bohr magnetons the energy is given in Rydbergs.

The temperature dependence of the inverse susceptibility (at a fixed volume) can be written as:

$$\chi(T)^{-1} = A + 5B\langle m^2\rangle + 35C\langle m^2\rangle^2 \tag{2.2}$$

where A, B, and C are the Landau coefficients and $\langle m^2\rangle$ is the mean square of the fluctuating magnetic moment. The latter quantity can be calculated by integrating over the wavevector-dependent susceptibility which is of the usual Ornstein–Zernike form. Integration can be carried out by introducing an *ad hoc* cut-off wavevector, corresponding to the long-wavelength (i.e. small-wavevector) limit. It has been shown (Mohn *et al* 1991) that $\langle m^2\rangle$ varies about linearly with temperature, so we can use the approximate relation:

$$\langle m^2\rangle = \alpha k_B T \qquad \text{with } \alpha = -B/(14Ck_B T_M) \tag{2.3}$$

Table 1. Crystallographic positions of the Pd shells surrounding the impurity. The distance between the shell and the impurity is given in units of the lattice constant a_0 of the 32-atom unit cell. The coordinate is given for one atom of the respective shell.

Shell	No of equivalent positions	Distance	Coordinate
1	12	$\sqrt{2}/4$	$\frac{1}{4}, \frac{1}{4}, 0$
2	6	1/2	$\frac{1}{2}, 0, 0$
3	24	$\sqrt{6}/4$	$\frac{1}{2}, \frac{1}{4}, \frac{1}{4}$
4	12	$1/\sqrt{2}$	$\frac{1}{2}, \frac{1}{2}, 0$
5	8	$\sqrt{3}/2$	$\frac{3}{4}, \frac{1}{4}, 0$

where α contains the unknown cut-off wavevector for the fluctuations. The proportionality constant α is determined to be $\alpha = 14.227\ \mu_B^2\ \mathrm{Ryd}^{-1}$ by requiring that the temperature of the susceptibility maximum agrees between theory and experiment (see section 5). For further details we refer to the references given above. In section 5 we will use (2.2) and (2.3) to determine the Curie temperature of the impurity system.

3. Band structure results for the Pd_{31}TM supercell

We choose a supercell of an FCC lattice consisting of 32 atoms to simulate an impurity in a Pd host. Figure 2 shows the 32-atom basis of the corresponding simple cubic Bravais lattice. The hatched circle is the impurity position, which is surrounded by five shells of Pd atoms, whose crystallographic positions are summarized in table 1. We note, however, that the polyhedron (first coordination shell in figure 2) is separated from the one in the neighbouring supercell by only half the lattice constant of the supercell, i.e. about 3.95 Å, but already the second coordination shell contains atoms from the neighbouring supercell. At present we neglect lattice relaxation effects around the impurity atom.

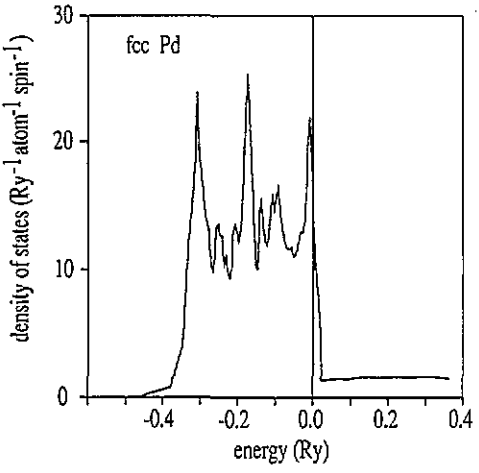

Figure 1. Total density of states (DOS) of FCC Pd.

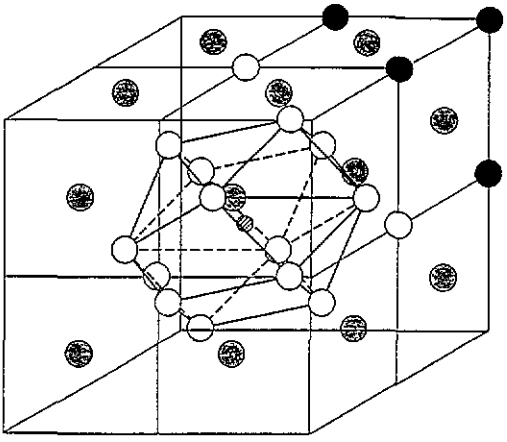

Figure 2. 32-atom basis of the simple cubic supercell of the TMPd_{31} structure. The impurity atom (hatched) is in the centre of the cell, the 12 first-nearest-neighbour atoms are plotted as a Pd_{12} ball and stick model. Atoms belonging to the same shell have equal shade of grey.

Our first-principles band structure calculations were performed self-consistently employing the augmented spherical wave (ASW) method by Williams *et al* (1979). Effects of exchange and correlation are treated within the local spin density approximation (LSDA) by von Barth and Hedin (1976) and Janak (1978). All calculations were performed using 35 k-points in the irreducible wedge of the Brillouin zone.

3.1. Density of states and corresponding magnetic moments

Figure 3 shows the DOS of all five impurity systems investigated. The Pd DOS (broken line) is averaged over all Pd atoms in the unit cell, which differ only slightly from each other and that of pure Pd, so introducing an impurity can be regarded as a small perturbation of the electronic structure of the host. It must be noted, however, that the presence of the impurity causes a small additional broadening of the Pd band width leading to a reduced height of the three pronounced peaks found in the DOS of the pure Pd (figure 1). Concerning the impurity we find that its interaction with the Pd host is significantly different for majority- and minority-spin electrons. While the former strongly hybridize, the latter form narrow localized bands mostly above the Fermi energy. This different behaviour is caused by the spin splitting of the impurity states leading to a *small* energy difference (favourable for interactions) between the impurity and the Pd states for *spin-up* electrons, so the respective impurity bands are about as broad as the host 4d bands. For *spin-down* electrons, however, this energy difference becomes too *large* for a strong interaction, so the respective states form narrow impurity bands around E_F.

This mechanism can already be seen for Cr**Pd**: the interaction is strong for the spin-up electrons, while for the spin-down electrons the orbital energy is much higher for Cr than for Pd, so the large energy difference causes a very weak interaction and thus a sharp peak in the DOS separated from the host d bands. We find an antiparallel coupling between the Cr moment and the host moment that makes the total moment per unit cell rather small. We note that Gainon and Sierro (1968) deduced from their experiments an antiferromagnetic interaction between the Cr impurity and the Pd host.

For Mn**Pd** the spin splitting is larger than in Cr**Pd**, leading to a spin magnetic moment of 3.96 μ_B for Mn. With its five d electrons, the Mn majority-spin band is full and completely hybridizes with the host spin-up electrons. The empty minority-spin bands of Mn are still separated from the host d bands and lead to a peak in the DOS above E_F. Although the Mn impurity moment is largest among the 3d transition metals, the relative polarization of the Pd host is very small, but already shows ferromagnetic coupling.

In the present series the largest total moment per cell (not per impurity) is found for Fe**Pd** and is 7.51 μ_B for the 32-atom cell. The effective orbital energy of the impurity atom is lowered with increasing nuclear charge and thus gets closer to the host band states causing a stronger broadening of the minority-spin states associated with the impurity. The Fe spin-down DOS has the impurity peak much closer to E_F than the previous cases and consequently the hybridization with the Pd host is stronger, increasing the DOS in the low-energy region.

Co**Pd** behaves similarly to Fe**Pd**, but the additional valence electron of Co occupies part of the spin-down impurity bands, so the magnetic moment is reduced to 2.15 μ_B. The relative polarization of Pd is further increased as a consequence of the reduced energy difference between the atomic host and the impurity states.

In Ni**Pd** the impurity atom Ni carries a magnetic moment of 0.84 μ_B, which is again higher than in bulk Ni. The relative polarization of Pd is largest for Ni**Pd** and the coupling is ferromagnetic. Since Ni and Pd belong to the same group, their d-electron orbital energies become comparable, so the hybridization is stronger than in all other cases. Experimental investigations on that system do not give a clear picture: Chouteau (1976) does not find

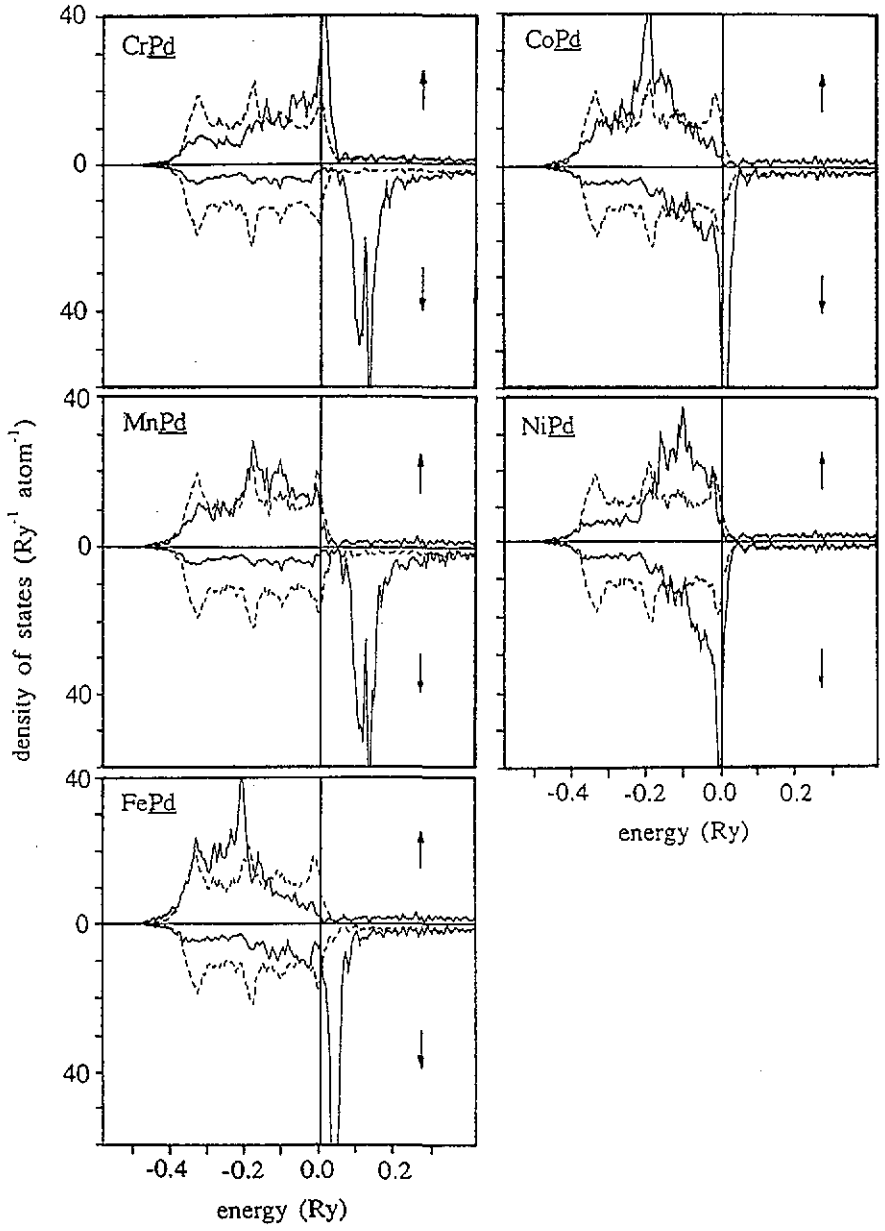

Figure 3. Densities of states of the five systems investigated. The full curves depict the impurity DOS, the dashed curve shows the host DOS averaged over all 31 Pd host sites.

any moment at Ni sites, whereas Loram and Mirza (1985) determine an impurity moment of about 1 μ_B.

3.2. Discussion of the magnetic moments

In table 2 we summarize our theoretical results related to magnetism and compare them with the cluster investigation of Oswald *et al* (1986), who performed calculations for an

infinite Pd crystal and studied the effects of a single impurity atom using perturbations of the potentials of the impurity and the first *three* Pd shells. This geometry leads to a cluster of 43 atoms embedded in an unperturbed Pd lattice. In the present calculation, we extend the interaction range up to *five* shells, but we use a supercell geometry with an underlying translational symmetry. Our cell contains one impurity among 32 atoms (representing an impurity concentration of 3.125 at.%), but not the infinitely diluted case, so (hopefully weak) interactions between the impurity atoms are present in our calculations. One should keep in mind this difference in models, when we compare their results with ours.

Table 2. M_{TM} is the magnetic moment of the transition metal impurity, Pd^n are the magnetic moments for the Pd atom in shell n, M_c is the magnetic moment for the 32-atom unit cell, $\langle M_{Pd}\rangle$ is the average magnetic moment per Pd atom, * denotes the respective values of Oswald *et al* (1986), M_{TM}^{exp} is the experimental impurity moment, M_g^{exp} is the experimental value of the giant moment extrapolated to zero impurity concentration. All moments are given in units of Bohr magnetons.

	M_{TM}	Pd^1	Pd^2	Pd^3	Pd^4	Pd^5	M_c	$\langle M_{Pd}\rangle$	M_{TM}^*	$\langle M_{Pd}^*\rangle$	M_{TM}^{exp}	M_g^{exp}
$Pd_{31}Cr$	2.86	−0.08	−0.10	−0.08	−0.15	−0.05	0.11	−0.088	3.14	−0.010	—	—
$Pd_{31}Mn$	3.96	0.05	0.02	0.04	−0.02	0.06	5.04	0.035	4.13	0.024	4–5	6.5–8
$Pd_{31}Fe$	3.29	0.16	0.15	0.12	0.11	0.12	7.51	0.136	3.47	0.049	3.5	10–12
$Pd_{31}Co$	2.15	0.19	0.17	0.15	0.17	0.14	7.41	0.170	2.28	0.055	2.1	9–10
$Pd_{31}Ni$	0.84	0.11	0.10	0.09	0.12	0.07	4.00	0.102	0.92	0.030	0–1	4.6

From table 2 we see that the impurity moments $\langle M_{TM}\rangle$ agree rather well between our supercell and the cluster calculation. This is not surprising, since earlier investigations have already shown, that this moment is fairly independent of the cluster size (Delley *et al* 1982, 1983). It should be noted, however, that the supercell approach systematically leads to smaller impurity and significantly larger Pd moments for the different shells than in the cluster calculation. The periodic array of supercells favours the long range magnetic interaction in Pd, a high-susceptibility system, and leads to an overlap of the polarization clouds around each single impurity and thus causes larger Pd moments.

By adding all contributions to the total moment within the $Pd_{31}TM$ supercell we obtain the cell moment $\langle M_c\rangle$ which is considerably smaller than the experimental 'giant moment'. The latter, however, is extrapolated to zero impurity concentration (see e.g. Bozorth *et al* 1961) and thus corresponds to a different physical situation than our theoretical result which is based on a 3.125 at.% simulation. Therefore we should use comparable impurity concentrations, but then our theoretical values agree much better with the corresponding experimental moments, namely $\simeq 7\ \mu_B$ for **CoPd**, and $\simeq 5$–$6\ \mu_B$ for **MnPd** taken from the review by Nieuwenhuys (1975), values that are very close to our cell moments.

The same sort of argument is valid for the cluster results; the cluster size of 43 atoms is not large enough to simulate the complete polarization cloud around a single impurity, a fact already stated by Oswald *et al* (1986). A recent reinvestigation of the **FePd** system, in which the cluster size was increased to 225 atoms (12 Pd shells), led to a total moment of 6.7 μ_B, still much smaller than the experimental giant moment. Therefore even 12 shells are not enough to contain the whole polarization halo (Zeller and Dederichs 1991) and thus all these results confirm the early observation, at least indirectly, that the polarization caused by the impurity should extend up to 200 Pd atoms (Low and Holden 1966). It is difficult to argue whether the supercell or the embedded cluster approach comes closer to the physical reality, but both models lead to a strong polarization of the Pd host which does not show any oscillations or a simple exponential decay (Low and Holden 1966).

3.3. The impurity moment

The impurity moment plotted as a function of the respective atomic number (dashed line in figure 4) shows a 'Hund's rule' rather than a Slater–Pauling behaviour where the maximum appears between Fe and Co (Schwarz *et al* 1984). This means that the localized impurity moment can be described in an atomic-like picture using magnetic quantum numbers (Nieuwenhuys 1975) with its maximum value for the half-filled d-band (figure 4). The magnetic moment per cell M_c is given by the impurity moment M_{TM} plus the host polarization M_{Pd} of the 31 surrounding Pd atoms. We find a smooth parabolic curve, which has its maximum between Fe and Co in agreement with experiment.

Another interesting result is obtained by plotting the relative polarization M_{Pd}/M_{TM} as a function of d-shell filling Z_d of the impurity atom (full line of figure 4). We—in agreement with the cluster results—find a perfect linear relation showing that the ability of an impurity atom to polarize the host electrons decreases, when the orbital energy difference between impurity and host increases. Phenomenologically this is easy to understand: the polarization of the host lattice is caused by the covalent interaction between the spin-split states of the impurity and the host atoms (Anderson 1961, Wolff 1961, Clogston 1961, Moriya 1965). Apart from the magnitude of the overlap between the impurity and host wave functions, the strength of the covalent interaction depends on the magnitude of the energy difference between the respective host and impurity states. The almost completely filled 4d band of the Pd host creates a strongly repulsive potential which causes a narrow band close to the Fermi energy originating from the impurity states (Friedel 1958). This effect is strongest for impurity atoms at the beginning of a d series and gradually weakens when the number of the impurity valence electrons Z_d is increased, since the orbital energy difference between the host and impurity atom decreases making the covalent interaction stronger. If the impurity states split magnetically, this energy difference becomes smaller for the majority states and larger for the minority states. This brings us back to what has been discussed in connection with the DOS displayed in figure 3, where we have already described why the hybridization between the majority-spin is much stronger than for the minority-spin states.

This interpretation explains why the relative polarization is strongest for the Ni impurity. The antiparallel polarization found in the Cr**Pd** system requires a more detailed analysis. The DOS of Cr**Pd** is dominated by two major structures (figure 3): In the minority-spin case the impurity forms localized bands with a peak in the DOS which is about 1.5 eV above E_F; the majority-spin states associated with the impurity are characterized by narrow bands with a DOS peak at and just above the Fermi energy. The hybridization in the majority bands dominates the polarization, while the covalent interactions in the minority bands are weak. The covalent interactions near E_F push some spin-up Pd states above E_F and consequently cause states with Cr character below E_F. Thus this reduction in spin-up Pd states together with the largely unperturbed spin-down Pd bands is responsible for the antiparallel polarization found in Cr**Pd**. In the following chapter we will present a model for this so called 'covalent polarization'.

4. The model of covalent polarization

The interaction between the localized impurity states and the host bands leads to an induced magnetic moment at the host atoms. This 'covalent polarization' was already described in the early impurity models (Anderson 1961, Wolff 1961, Clogston 1961, Moriya 1965). The behaviour of 3d impurities in Ni was discussed extensively by Friedel (1958). A tight bonding model, very similar to the one presented here, was given by Kanamori (1965). For

magnetic alloy systems the concept of 'covalent magnetism' was proposed by Williams *et al* (1981) as an alternative approach to the Stoner model.

In our covalent polarization (CP) model we study the interaction of a localized impurity state at E_0, that is spin-split (labelled $E^{\uparrow}$ and $E^{\downarrow}$) and interacts with a paramagnetic host, whose electronic structure is crudely represented by a density of states of rectangular shape with $N(E) = N_0$. In figure 5 we sketch such a situation, where we choose the bottom of the host band as energy zero and indicate the Fermi energy E_F. The strength of interaction is controlled by an electron hopping term t. We assume that the localized impurity states interact with the band states of the host forming a bonding state (E_1) and an antibonding state (E_2), where the occupation of these states is given by the square of the respective eigenvectors. This covalent interaction modifies the DOS for host and impurity states. Separate integration over all occupied states of this new host DOS for spin-up and spin-down electrons yields the host moment M_{CP} caused by the covalent interaction between host and impurity:

$$M_{CP} = \frac{t}{2}N(E_F)\left(\tan^{-1}\left(\frac{E^{\downarrow}}{2t}\right) - \tan^{-1}\left(\frac{E^{\uparrow}}{2t}\right) - \tan^{-1}\left(\frac{E^{\downarrow} - E_F}{2t}\right) + \tan^{-1}\left(\frac{E^{\uparrow} - E_F}{2t}\right)\right). \tag{4.1}$$

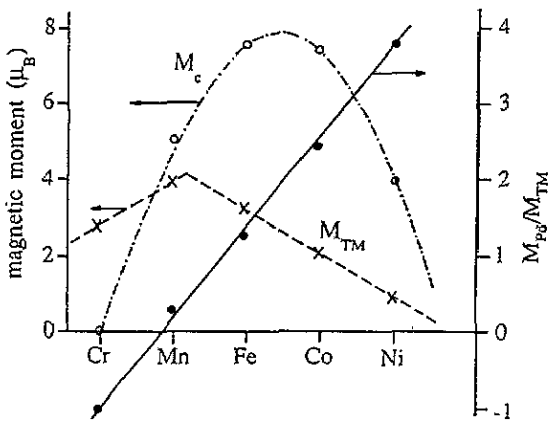

Figure 4. Magnetic moment of the 32-atom unit cell M_c (dashed-dotted curve; open circles), magnetic moment of the impurity atom M_{TM} (dashed curve; crosses), and the relative polarization M_{Pd}/M_{TM} (full curve; full circles) as a function of the atomic number of the impurity atom.

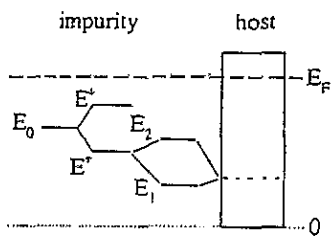

Figure 5. Sketch of the model used to derive the covalent polarization. E_0 is the non-magnetic impurity level, which is spin split into $E_{\uparrow}$ and $E_{\downarrow}$. These two states interact with the host band structure depicted by the rectangular density of states.

In this simple model we have neglected exchange effects so that M_{CP} is the moment, which in the actual system will be multiplied by a Stoner enhancement factor S coming from the host electrons (Moriya 1965). In order to discuss the properties of the CP model we expand the $\tan^{-1}(x)$ up to the third power in x and obtain:

$$M_{CP} = -[N(E_F)/(16t^2)]E_F I_1 M_1(E^{\uparrow} + E^{\downarrow} - E_F). \tag{4.2}$$

In (4.2) we have replaced the exchange-splitting of the impurity state, $E^{\uparrow} - E^{\downarrow}$, by its magnetic moment M_I times the respective Stoner exchange factor I_I. With the non-magnetic impurity level E_0 defined by

$$E_0 = (E^{\uparrow} + E^{\downarrow})/2 \tag{4.3}$$

we obtain

$$M_{CP} = -[N(E_F)/(8t^2)]E_F I_I M_I (E_0 - E_F/2). \tag{4.4}$$

Although we have used some rather crude assumptions, such as a fully localized impurity state and a rectangular DOS for the host, equation (4.4) qualitatively and semi-quantitatively describes the essential properties of both, band structure calculation and experiment. The introduction of a more realistic band structure (i.e. DOS) of the host lattice would only affect the energy for which the RHS of (4.4) vanishes, but the trends will remain, so that the simple CP model contains the basic physics. Therefore we can summarize the qualitative behaviour of the system by discussing M_{CP} in comparison to the band structure results:

(i) if E_0 lies above $E_F/2$, the polarization of the host lattice is antiparallel to the impurity moment as in the Cr**Pd** system;

(ii) if E_0 comes close to $E_F/2$, the polarization becomes very small as in Mn**Pd**;

(iii) if E_0 becomes progressively smaller (when going from Mn towards Ni), M_{CP} increases and stays positive.

We obtain the ratio of the relative polarization between the host (M_H) and the impurity moment (M_I) within the CP model as

$$\frac{M_H}{M_I} = S\frac{M_{CP}}{M_I} = -\chi_H \frac{E_F}{8t^2}\frac{I_I}{I_H}\left(E_0 - \frac{E_F}{2}\right) \tag{4.5}$$

where χ_H is the paramagnetic susceptibility of the host, E_F is determined by the host, and I_I and I_H are the Stoner exchange factors of impurity and host, respectively. We notice that the RHS of (4.5) no longer depends on the value of the impurity moment, M_I. The relative polarization M_H/M_I scales with the value of E_0, which varies about linearly from Cr towards Ni and thus is responsible for the linear behaviour of M_{Pd}/M_I shown in figure 4. Van Acker *et al* (1991) came to the same conclusion on the basis of a generalized Clogston–Wolff (CW) model. Our quantity E_0 is closely related to a the non-magnetic potential used in the CW model (see figure 7, van Acker *et al* 1991), both of which vary about linearly with the atomic number of the impurity.

5. The Curie temperature of impurity systems

In the previous chapters we pointed out that the magnetic behaviour of these impurity systems is characterized by the coexistence of partly localized and itinerant electrons. Bloch *et al* (1975) showed very elegantly how to treat such basically different magnetic states in one formalism. These authors explained the magnetic behaviour of the Laves phase compounds $RECo_2$, where the rare earth (RE) atoms possess the magnetic moments from their localized 4f electrons, which interact with the itinerant 3d electrons of Co. Their model can be adapted to the present impurity problem where we find a similar situation, since the

magnetic moments of the impurity atoms are rather localized and interact with the itinerant 4d electrons of the Pd host.

Early attempts to theoretically determine the Curie temperature T_c in the present systems were undertaken by Takahashi and Shimizu (1965), by Kim (1966) and Long and Turner (1970), but in all three models T_c was found to be proportional to the impurity concentration in contrast to experiment.

We therefore suggest an improved model for computing Curie temperatures and start with the formulation of the Gibbs free energy of a system consisting of localized (impurity) and itinerant (host) electrons with the respective magnetic moments as given by Bloch *et al* (1975) and Takahashi and Shimizu (1965), but then we generalize the model by introducing the thermal dependence of the host susceptibility, which is governed by spin fluctuations (Mohn and Schwarz 1992). With these assumptions we derive an expression for the inverse susceptibility which now contains the effects of the localized impurity moments (via a Weiss mean field model) and the effects of thermal spin fluctuations analogous to an approach by Murata and Doniach (1972). In appendix A we sketch the derivation of (A13):

$$A + 5B\alpha k_B T_c + 35C\alpha^2 k_B^2 T_c^2 = [(g-1)^2/\mu_B^2 N] I_0^2 [J(J+1)/3k_B T_c]$$

from which the Curie temperature can be obtained. All quantities entering (A13) can be derived from band structure results of the undisturbed host lattice and the impurity system and thus are determined from first principles. Only the proportionality constant α is adjusted to experimental data, namely the temperature variation of the susceptibility of *pure* Pd as described in section 2.

We enter the values for A, B, C, and α from our calculation of pure FCC Pd in order to evaluate (A13), but when we try to use the magnetic moments from the supercell calculation, we obtain Curie temperatures which are much too high. Only when we take the magnetic moments from the cluster calculations by Oswald *et al* (1986), we obtain good agreement with the concentration dependence of T_c determined experimentally. In figure 6 we show the results of such a model for the Curie temperature of MnPd, FePd, and CoPd, where the experimental data were taken from Niuwenhuys (1975). The concentration dependence was introduced by assuming that for small concentrations the field acting on the host lattice, which is due to the covalent polarization is proportional to the number of impurity atoms.

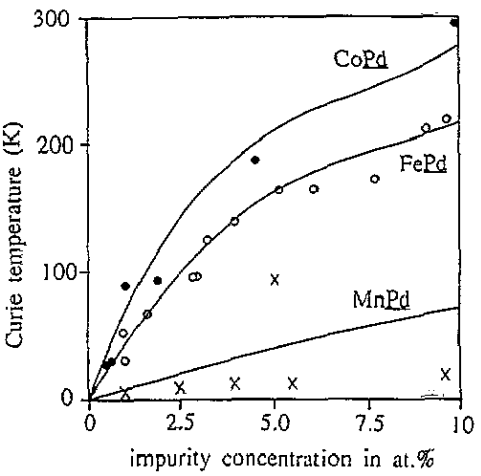

Figure 6. Concentration dependence of the Curie temperature for MnPd, FePd, and CoPd calculated from (A13) (solid curves) in comparison with experiment. The experimental values are given by crosses for MnPd, open circles for FePd and full circles for CoPd.

The deviation in T_c from linearity found for FePd and CoPd is caused by the temperature dependence of the inverse susceptibility of the Pd host (LHS of (A13)) and the concentration

dependence of the coupling constant I_0 via the field H_{Pd} (see (A14) in appendix A). It is somewhat surprising that this simple model agrees so well with experiment to concentrations up to an impurity concentration of 10%. Only for MnPd we find a large discrepancy between our simple model and the experimental T_c for concentrations exceeding 3% impurities, but this may be related to the spin glass behaviour of MnPd which starts around that concentration (Coles *et al* 1975).

Despite the success of this simple model it should be noted that T_c depends sensitively on the details of the band structure (and its method of calculation) especially for a high susceptibility system such as Pd. Nevertheless, the spin fluctuations used in our model adequately describe the deviation from linearity of T_c as a function of the impurity concentration in contrast to earlier models.

6. Conclusion

The supercell calculations presented in this work describe the electronic and magnetic structure of the TMPd systems fairly well. We find localized moments at the 3d impurity atoms and a polarization of the surrounding host Pd atoms which results in the 'giant moments' observed experimentally, but the overlap of the polarization cloud leads to higher moments than in cluster results. The coupling between the impurity moment and the host is ferrimagnetic for CrPd and ferromagnetic for all other 3d metals investigated. For an explanation of this coupling we present the CP model which is based on a covalent interaction between the impurity atom and the host and can qualitatively explain the band structure results. In order to estimate the concentration dependence of the Curie temperature in these impurity systems we modify the model of Bloch *et al* (1975) by introducing the effect of spin fluctuations of the Pd host. The calculated values of T_c agree well with experiment provided the induced moments are taken from the cluster approach of Oswald *et al* (1986). We conclude that the translational symmetry assumed in the present supercell calculation together with the high susceptibility of the Pd host leads to an enhancement of the host polarization, which was not found in the cluster calculation. Supercell calculations for systems with a smaller susceptibility like Ag should thus not show this shortcoming of this approach.

Acknowledgment

The extremely time consuming supercell calculations were carried out at the IBM ES9000 computer of the Vienna University Computing Centre within the European Academic Supercomputing Initiative (EASI) sponsored by IBM.

Appendix A

The localized magnetic moment of the impurity M_I is proportional to an angular momentum J and is given by the relation

$$M_I = \mu_B g J. \tag{A1}$$

The impurity moment couples to the Pd spin s via a term

$$2I_0(g-1)J \cdot s. \tag{A2}$$

In (A1) and (A2), J is the total angular momentum of the impurity, g, the Landé factor, s the Palladium spin, and I_0 a coupling constant that will be determined later. The Hamiltonian for such a system with an external field H applied in the z direction is given by

$$H = H_b + [2I_0(g-1)\langle s_z\rangle + g\mu_B H]\sum_i J_i^z + 2N\mu_B\langle s_z\rangle H \tag{A3}$$

where H_b is the electronic 'band structure' contribution, $\langle s_z\rangle$ the average spin in the Pd 4d band and N the number of impurity atoms per molecular unit, respectively. The magnetization of the Pd host is

$$M_{Pd} = -2N\mu_B\langle s_z\rangle. \tag{A4}$$

From (A3) we derive H_I the 'molecular field' which acts on the localized impurity moments and represents the influence of the itinerant Pd spins via a coupling parameter I_0

$$H_I = H - [(g-1)/g\mu_B^2 N]I_0 M_{Pd}. \tag{A5}$$

The Gibbs free energy contains the Helmholtz free energy of the Pd host $F_{Pd}(M_{Pd}, T)$, the contribution of the external field $-HM_{Pd}$ and the usual term in the Weiss model for an angular momentum J in a molecular field H_I:

$$G = F_{Pd}(M_{Pd}, T) - HM_{Pd} - Nk_BT\ln(\sinh((J+\tfrac{1}{2})y)/\sinh(y/2)) \tag{A6}$$

with

$$y = (g\mu_B H_I)/(k_B T). \tag{A7}$$

From the equilibrium condition $\partial G/\partial M_{Pd} = 0$ we obtain

$$-\partial F_{Pd}(M_{Pd}, T)/\partial M_{Pd} = H - [(g-1)/\mu_B]I_0 J\mathcal{B}_J(Jy) \tag{A8}$$

where the Brillouin function $\mathcal{B}_J(Jy)$ is defined as

$$\mathcal{B}_J(Jy) = \frac{2J+1}{2J}\coth((J+\tfrac{1}{2})y) - \frac{1}{2J}\coth\left(\frac{y}{2}\right). \tag{A9}$$

With the usual high temperature expansion of $\mathcal{B}_J(Jy)$

$$\mathcal{B}_J(Jy) \simeq \tfrac{1}{3}y(J+1) \tag{A10}$$

and for zero external field, $H = 0$, we obtain

$$\frac{\partial F_{Pd}(M_{Pd}, T)}{\partial M_{Pd}} = \frac{(g-1)^2}{\mu_B^2 N} I_0^2 \frac{J(J+1)}{3k_B T} M_{Pd}. \tag{A11}$$

The RHS side of (A11) renormalizes the coefficient $A(T)$ of the free energy $F_{Pd}(M_{Pd}, T)$ that the equilibrium condition (A8) reads:

$$0 = \frac{\partial G}{\partial M_{Pd}} = M_{Pd}\left(-A(T) + \frac{(g-1)^2}{\mu_B^2 N} I_0^2 \frac{J(J+1)}{3k_B T}\right) + \ldots. \tag{A12}$$

The coefficient $A(T)$ is the inverse susceptibility of the host, which would show a linear increase with temperature (Curie–Weiss behaviour) for an ordinary paramagnetic host. For FCC Pd, however, the susceptibility shows a maximum around 90 K and the Curie–Weiss behaviour is only found for higher temperatures due to spin fluctuations as discussed recently (Mohn and Schwarz 1992). The temperature dependence of the Pd susceptibility is given by (2.2) and (2.3) which lead to an expression for the Curie temperature. Since the coefficient of M_{Pd} in (A12) must vanish at T_c we obtain a cubic equation in T_c

$$A + 5B\alpha k_B T_c + 35C\alpha^2 k_B^2 T_c^2 = \frac{(g-1)^2}{\mu_B^2 N} I_0^2 \frac{J(J+1)}{3k_B T_c}. \tag{A13}$$

For the systems investigated (A13) always has two imaginary and one real root, which determines T_c. In the case of three real roots, the root with a negative temperature derivative of the inverse susceptibility defines T_c.

The coupling constant I_0 can be determined from (A8) by setting $T = 0$, where $\mathcal{B}_J(Jy) = 1$, so that we obtain:

$$I_0 = \frac{\mu_B}{J(g-1)} \frac{\partial F_{Pd}(M_{Pd}, T=0)}{\partial M_{Pd}} = \frac{\mu_B}{J(g-1)} H_{Pd}. \tag{A14}$$

In (A14) we have introduced the quantity H_{Pd} which is the field acting on the Pd atom via the covalent polarization of the impurity. It has been shown, (Mohn and Schwarz 1992) that in Pd spin fluctuations cause a maximum in the susceptibility and are responsible for a deviation from linearity of the M versus H relation. Therefore H_{Pd} cannot simply be replaced by $H_{Pd} = M_{Pd}/\chi_{Pd}$, where χ_{Pd} is the paramagnetic susceptibility, but H_{Pd} must be expanded in a power series up to M_{Pd}^5. For an ordinary paramagnetic system, where the linear relation between magnetic field and magnetic moment holds, the coupling constant becomes

$$I_0 = M_{host}\chi_{host}^{-1}/[g(g-1)M_{imp}]. \tag{A15}$$

By comparing (A15) with (4.5) (the relative polarization from the CP model) we see that in both approaches the ratio M_{host}/M_{imp} is directly proportional to the host susceptibility, in agreement with physical intuition.

References

Anderson P W 1961 *Phys. Rev.* **124** 41

Bloch D, Edwards D M, Shimizu M and Voiron J 1975 *J. Phys. F: Met. Phys.* **5** 1217

Bozorth R M, Wolff P A, Davies D D, Compton V B and Wernick J H 1961 *Phys. Rev.* B **122** 1157

Cable J W, Wollan E O and Koehler W C 1965 *J. Appl. Phys.* **34** 1189

Chouteau G 1976 *Physica* B **84** 25

Clogston A M 1961 *Phys. Rev.* **125** 439

Coles B R, Jamieson H, Taylor R H and Tari A 1975 *J. Phys. F: Met. Phys.* **5** 565

Delley B, Ellis D E and Freeman A J 1982 *J. Magn. Magn. Mater.* **30** 71

Delley B, Jarlborg T, Freeman A J and Ellis D E 1983 *J. Magn. Magn. Mater.* **31–4** 549

Friedel J 1958 *Nuovo Cimento Suppl.* **2** 287

Gainon D and Sierro J 1968 *Phys. Lett.* **26A** 601

Janak J F 1978 *Solid State Commun.* **25** 53

Jarlborg T and Freeman A J 1981 *Phys. Rev.* B **23** 3577

Kanamori J 1965 *J. Appl. Phys.* **36** 929

Kim D J 1966 *Phys. Rev.* **149** 434
Kirchner B, Weber W and Voitländer J 1992 *J. Phys.: Condens. Matter* **4** 8097
Long B D and Turner R E 1970 *J. Phys. C: Solid State Phys.* **3** S127
Loram J W and Mirza K A 1985 *J. Phys. F: Met. Phys.* **15** 2213
Low G G and Holden T M 1966 *Proc. Phys. Soc.* **89** 119
Mohn P and Schwarz K 1992 *J. Magn. Magn. Mater.* **104–7** 685
Mohn P, Schwarz K and Wagner D 1989 *Physica* B **161** 153
—— 1991 *Phys. Rev.* B **43** 3318
Moriya T 1965 *Prog. Theor. Phys.* **34** 329
Murata K K and Doniach S 1972 *Phys. Rev. Lett.* **29** 285
Nieuwenhuys G J 1975 *Adv. Phys.* **24** 515
Ododo J C 1985 *J. Phys. F: Met. Phys.* **15** 941
Oswald A, Zeller R and Dederichs P H 1986 *Phys. Rev. Lett.* **56** 1419
Schwarz K and Mohn P 1984 *J. Phys. F: Met. Phys.* **14** L129
Schwarz K, Mohn P, Blaha P and Kübler J 1984 *J. Phys. F: Met. Phys.* **14** 2659
Takahashi T and Shimizu M 1965 *J. Phys. Soc. Japan* **20** 26
van Acker J F, Speier W and Zeller R 1991 *Phys. Rev.* B **43** 9558
von Barth U and Hedin L 1972 *J. Phys. C: Solid State Phys.* **5** 1629
Wagner D 1989 *J. Phys.: Condens. Matter* **1** 4635
Williams A R, Kübler J, Gelatt C D Jr 1979 *Phys. Rev.* B **19** 6094
Williams A R, Moruzzi V L, Kübler J and Schwarz K 1984 *Bull. Am. Phys. Soc.* **29** 278
Williams A R, Zeller R, Moruzzi V L, Gelatt C D Jr and Kübler J 1981 *J. Appl. Phys.* **52** 2067
Wohlfarth E P and Rhodes P 1962 *Phil. Mag.* **7** 1817
Wolff P A 1961 *Phys. Rev.* **124** 1030
Zeller R and Dederichs P H 1991 private communication